

Estimating Forest Carbon Stocks Using CNN and Vegetation Texture Features Extracted from UAV and Satellite Data in Telkom University

Raditya Aydin, Erwin Budi Setiawan

Informatics, Faculty of Informatics, Universitas Telkom, Bandung 40257, Indonesia

ARTICLE INFO

Article history:

Received December 04, 2024

Revised January 11, 2025

Accepted January 31, 2025

Keywords:

Carbon Stock Estimation;
Remote Sensing;
Convolutional Neural Networks;
Vegetation and Texture Features;
UAV and Satellite Data

ABSTRACT

Forests play a crucial role in mitigating climate change by acting as carbon sinks, yet traditional methods of carbon stock estimation, reliant on manual tree measurements, are costly, time-consuming, and geographically limited. Recent advancements in remote sensing technologies, such as the combination of Unmanned Aerial Vehicles (UAVs) and Google Earth Engine (GEE), offer a promising alternative by integrating high-resolution local observations with global-scale data. Using the power of Convolutional Neural Networks (CNNs), this study suggests an integrated method for classifying carbon stocks by fusing textural parameters like homogeneity and entropy with spectral indices like Green Chromatic Coordinates (GCC) and Excess Green Index (ExG). CNNs are used to capture the spectral richness and structural complexity of vegetation because of their propensity to extract hierarchical spatial characteristics. The research compares the performance of various feature combinations—color-based, texture-based, and mixed features—using a hybrid framework of UAV and GEE data. It is anticipated that the results will demonstrate how spectral and textural features work together to increase classification accuracy. In addition to tackling major issues in carbon stock estimation, this scalable and integrated framework is made to adapt to a variety of forest ecosystems and aid in the creation of conservation policies and the mitigation of climate change.

This work is licensed under a [Creative Commons Attribution-Share Alike 4.0](https://creativecommons.org/licenses/by-sa/4.0/)



Corresponding Author:

Raditya Aydin, Informatics, Faculty of Informatics, Universitas Telkom, Bandung 40257, Indonesia
Email: radityaaydin@student.telkomuniversity.ac.id

1. INTRODUCTION

Forests are an important aspect in mitigating the impacts of climate change because they act as carbon sinks, absorbing and storing carbon dioxide from the atmosphere [1], [2], [3]. Monitoring, reporting, and policy-making efforts to lower greenhouse gas emissions depend on accurate assessments of carbon stocks [4], [5]. The manual tree measurements used in traditional carbon stock calculation methods are expensive, time-consuming, and have a restricted geographic coverage [5], [6]. According to recent estimates, between 1988 and 2014, Russian woods stored about 354 teragrams (Tg) of carbon annually. This number, which is noticeably 47% greater than what was previously recorded in national inventories, shows how much carbon these forests can store because of their higher biomass density and larger forest area.

The combination of Unmanned Aerial Vehicles (UAVs) and Google Earth Engine (GEE) has emerged as a promising remote sensing technology advancement that could help overcome the drawbacks of traditional approaches. A supplementary dataset for tracking vegetation dynamics is made possible by GEE's broad, global-scale coverage and UAVs' high-resolution, localized observations [7], [8]. Higher spatial resolution carbon stock estimations can be obtained by researchers by utilizing both approaches, particularly in remote or intricate forest environments [9], [10]. For instance, merging GEE and UAV data enables the integration of

large-scale geographical patterns with fine-grained vegetation data, which is crucial for precise and scalable carbon monitoring [11], [12], [13]. Studies have demonstrated that GEE and UAVs have different color and texture extraction characteristics. GEE often uses conventional methods to isolate and transform raw data into a set of measurable attributes that can be used for further analysis, a process known as feature extraction techniques that may not be able to capture the same level of detail in texture analysis, where UAV-based uses advanced algorithms to improve classification accuracy [14], [15]. Therefore, combining the different properties of these two data will be a contribution that can support similar research in the future.

Convolutional Neural Networks (CNN), in particular, are deep learning models that have proven to be efficient tools for evaluating data from GEE and UAVs. CNNs excel at extracting hierarchical spatial properties, which describe CNNs' capacity to identify patterns at various granularities, including edges, forms, and intricate structures in pictures and makes them ideal for tasks involving images, such as classification and segmentation [16]. Previous research has demonstrated the ability of CNNs in biomass estimation, with a good R^2 value of 0.943 [8].

CNN models outperformed conventional machine learning techniques in previous studies on individual tree biomass estimation in natural secondary forests using WorldView-3 images and aerial laser scanning (ALS) data, with RMSE values ranging from 7.47 kg to 36.83 kg and R^2 values between 0.68 and 0.85 [17]. Precision forestry and carbon management techniques were advanced by the combination of ALS with high-resolution photography, which increased classification accuracy and gave comprehensive spatial AGB distribution. The integration of spectral and texture information, the requirement for sizable labelled datasets, and the dangers of overfitting persist despite CNNs' ability to detect spatial patterns [16]. In order to improve CNN's scalability and generalization across various forest types, settings, and regions in carbon stock estimation, these problems must be resolved.

For non-spatial data analysis, Multilayer Perceptrons (MLP) have been employed extensively in addition to CNNs. Although MLP works well with numerical and categorical data, it is not as useful for tasks like carbon stock estimation because it cannot capture the spatial hierarchy of image data. Nonetheless, a hybrid strategy that combines MLPs for examining supplementary spectral or textural characteristics with CNNs for extracting spatial features may have a great deal of promise for increasing prediction accuracy [18], [19].

In the calculation of carbon stocks based on remote sensing, feature extraction is essential. Green Chromatic Coordinates (GCC), Color Vegetation Index (CVI), and Excess Green Index (ExG) are a few examples of vegetation indicators that offer useful spectral data about biomass and vegetation health. In a similar vein, texture attributes such as homogeneity, contrast, and entropy provide information on structural complexity and spatial patterns, both of which are connected to carbon storage capability [20], [21]. Although previous studies have demonstrated that each of these traits can increase prediction accuracy on its own, little is known about how to integrate and use them with CNNs [22], [23].

This study fills a major gap in current approaches by evaluating the integration of color and texture information with CNNs for carbon stock classification. It does this by investigating the best way to combine spectral and spatial characteristics to increase classification accuracy. In contrast to earlier research that concentrated on texture features like homogeneity, contrast, and entropy or spectral indices like ExG, CVI, and GCC independently, this study employs CNN architecture to capture the structural complexity and spectral richness of vegetation by integrating these features into a single, unique framework. Furthermore, this study aims to determine the most effective method for classifying carbon stocks by methodically comparing the performance of several feature combinations, including color-based, texture-based, and mixed features. This research is a new addition to the field of remote sensing-based carbon stock estimation, as it contributes to the development of an integrated approach that combines spectral and textural features for carbon stock classification, identifies the most effective classification method by comparing feature combinations, and proposes a scalable framework that combines UAV and GEE data for applications in various forest ecosystems. As far as the authors are concerned, in order to classify carbon stocks, the majority of previous research either only looks at textural features or spectral indices, without merging the two in a cohesive manner. By connecting local high-resolution observations with global-scale data, the complementing datasets from UAVs and GEE enhance this research and provide a precise and scalable approach that can be tailored to different forest ecosystems. In addition to increasing the precision of carbon stock monitoring, this novel framework is anticipated to be a significant step in the development of dependable and scalable approaches to tackle climate change issues and guide conservation policies.

2. METHODS

This section describes the methodical process used in this study to create and assess a machine learning-based framework for classifying carbon stocks. Data collection, preprocessing, feature extraction, and

convolutional neural network (CNN) classifier implementation are all included in the techniques. The work intends to solve issues like data imbalance and model overfitting while overcoming the drawbacks of conventional carbon stock estimating techniques by utilizing remote sensing data and combining spectral and textural properties. The thorough approach guarantees the research's reproducibility and lays the groundwork for future developments in this field.

2.1. Proposed Method

The research method that will be carried out will go through several stages as can be seen in Fig. 1. Data gathering, which includes field carbon stock assessments, drone data, and Google Earth Engine (GEE) data, is the first step in the technique. To guarantee that the dataset labelling is accurate and that the geographic properties of the GEE and UAV data are aligned, field data is utilized. Following data gathering, a data labeling procedure is carried out to give the photos carbon stock values derived from field measurements. Data cleaning is the next step, which eliminates noise and irregularities that could impair model performance.

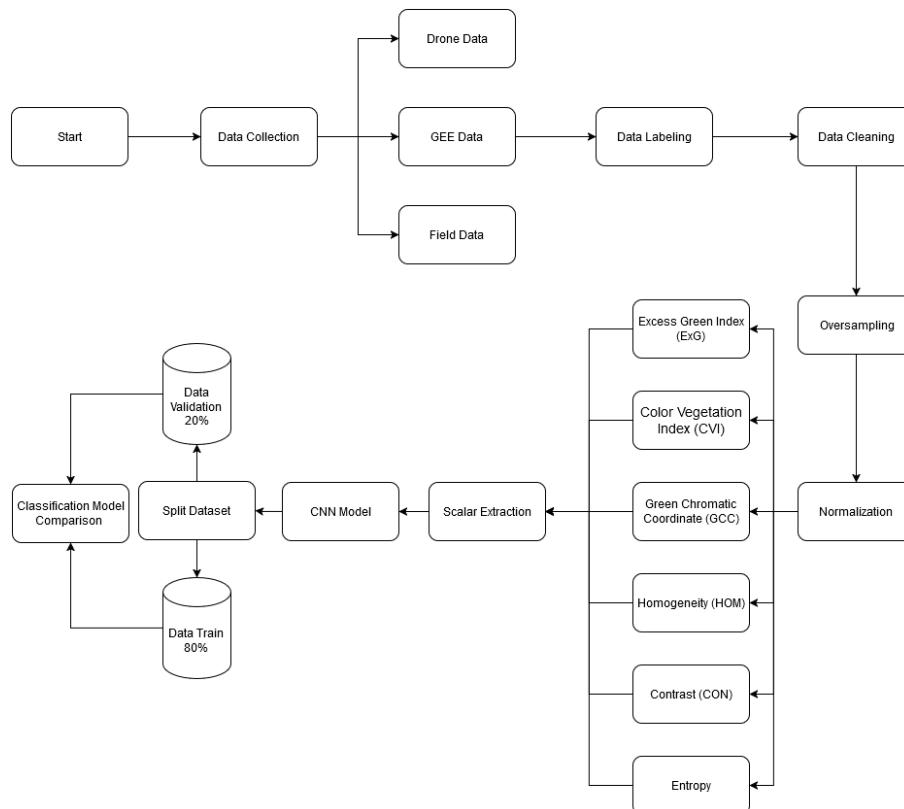


Fig. 1. Research methodology flowchart

In order to rectify class imbalances and guarantee that minority classes—such as low and high carbon stocks—are fairly represented, the cleaned dataset is oversampled. In order to standardize the feature values and provide consistent input for machine learning models, a normalization phase comes next.

Six essential features—the Excess Green Index (ExG), Color Vegetation Index (CVI), Green Chromatic Coordinates (GCC), Homogeneity (HOM), Contrast (CON), and Entropy—are extracted from the photos during the feature extraction phase. In order to obtain spectral and geographic data about vegetation properties and carbon stock levels, these features are extracted.

The dataset is divided into 80% for training and 20% for validation following feature extraction. A CNN model processes the training data for feature learning, and scalar extraction is used to separate and examine the contributions of individual features or feature combinations. Both scalar characteristics and image data can be integrated into the CNN framework using this multi-input method.

In order to choose the best features for precise carbon stock categorization, the trained CNN model is lastly assessed and contrasted across several feature extraction scenarios. The process makes use of both UAV and GEE data to offer a reliable and scalable carbon stock assessment solution.

2.2. Dataset Preparation

In addition to collecting image data using GEE and drones, field carbon stock data was obtained directly from Telkom University in Bandung, Indonesia. The main guideline for data collection, the Indonesian National Standard (SNI) for Carbon Stock Measurement and Estimation, formed the basis for the entire data collection mechanism. Telkom University provided six plots in total. These plots were obtained by dividing the 20m×20m dimension into four subplots: Sub-plot A (1m×1m). Sub-plots B, C and D were 5m×5m, 10m×10m and 20m×20m respectively as seen in Fig 2. Each of these sub-plots contained the samples required for carbon accounting as stated in SNI [24].

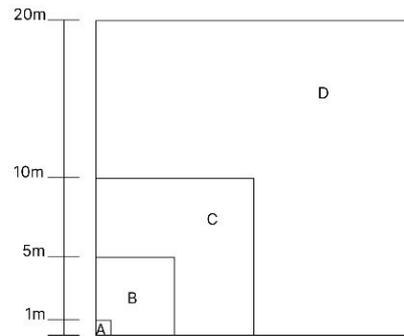
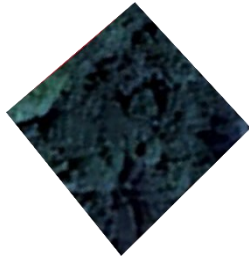


Fig. 2. SNI carbon measurement plot

The ZxHxPx naming system was used to identify the seedling and understorey biomass from each plot, which was then measured for wet weight (±300 grams) using pre-made sample containers. The samples were then taken to the lab so that the carbon content could be measured. During field data collection, coordinates were taken at each plot center in order to match plot conditions with Google Earth Engine satellite photos. A 20 MP Hasselblad L1D-20c camera with Hasselblad Natural Color Solution (HNCS) technology for spectrally correct imagery was mounted on a DJI Mavic 2 Pro drone to take aerial photos. To match ground plot sizes, plot photos from Google Earth Engine and drones were cropped and edited. Table 1 shows the file naming format rules such as source (1 means data from drone & 2 means data sourced from GEE), plot name, and carbon count.

Table 1. Sample of dataset

Dataset	Dataset Label	Carbon Ammount (kg)
Drone	 1-Z2H1P1-8365	8.365
GEE	 2-Z4H1P1-2826	2.826 kg

These data were then divided into classes: high, medium and low following the recommendations provided by the Ministry of National Development Planning/National Development Planning Agency of the Republic of Indonesia (BAPPENAS) [25].

The dataset was then staged and classified into three carbon classes: high, medium and low [25]. This classification was done at various plot sizes, such as 1×1 m, 5×5 m, 10×10 m, and 20×20 m, to ensure that the analysis was organized at different levels of granularity.

In Sub-Plot A (1×1 m), the high category was defined by a carbon weight greater than 54 kg (Drone) or greater than 42 kg (GEE), while the stationary category was found in the weight range of 31-54 kg (Drone) and 20-42 kg (GEE). The weight range for this category was below or equal to 31 kg (Drone) and 20 kg (GEE).

For Sub-Plot B (5×5 m), carbon in the high category had values close to 1086 kg (Drone) or 1138 kg (GEE). The medium category is 503-1086 kg (drone) and 594-1138 kg (GEE), while the low category is below or equal to 503 kg (drone) and 594 kg (GEE).

In Sub-Plot C (1×10 m), the carbon weight in the high category was close to 4487 kg (Drone) or 4480 kg (GEE). The ranges 2467-4487 kg (Drone) and 2530-4480 kg (GEE) are the two categories. Carbon values in the low category are below or equal to 2467 kg (Drone) and 2530 kg (GEE).

Finally, as can be seen in Table 2, Sub-Plot D (20×20 m) used a combination of Drone and GEE data, with high categories for carbon weights greater than 18249 kg, medium categories for carbon values between 10339 and 18249 kg, and low categories less than or equal to 10339 kg. This classification is designed to facilitate carbon stock analysis based on data source and measurement scale, which can help decision-making in forest development and climate change mitigation.

Table 2. Dataset classification table

Sub-Plot	Low Class	Medium Class	High Class
A (1×1m)	≤ 31 Kg (Drone) ≤ 20 Kg (GEE)	31 – 54 Kg (Drone) 20 – 42 Kg (GEE)	> 54 Kg (Drone) > 42 Kg (GEE)
B (5×5m)	≤ 503 Kg (Drone) ≤ 594 Kg (GEE)	503 – 1086 Kg (Drone) 594 – 1138 Kg (GEE)	> 1086 Kg (Drone) > 1138 Kg (GEE)
C (10×10m)	≤ 2467 Kg (Drone) ≤ 2530 Kg (GEE)	2467 – 4487 Kg (Drone) 2530 – 4480 Kg (GEE)	> 4487 Kg (Drone) > 4480 Kg (GEE)
D (20×20m)	≤ 10339 Kg (Drone & GEE)	10339 – 18249 Kg (Drone & GEE)	> 18249 Kg (Drone & GEE)

With 1,105 samples in the Medium class, 665 in the High class, and 550 in the Low class, the initial class distribution in this study was unbalanced. In order to solve this, synthetic examples for the minority classes were created by applying SMOTE to the training data, particularly for the Contrast feature. With 884 samples in each class and a training data shape of (2652.1) for features and (2652.3) for labels, the class distribution was balanced when SMOTE was applied. By guaranteeing that the model is exposed to every class equally, this balancing enhances the model's capacity to generalize and produce precise predictions, especially for the minority classes [26], [27].

Following initial classification, key spatial and spectral properties were extracted from the dataset images by processing. Various feature extraction techniques were applied to each image in order to turn visual data into scalar representations. The Green Chromatic Coordinate (GCC), Color Vegetation Index (CVI), and Excess Green Index (ExG) were important metrics. Furthermore, vegetation density, texture uniformity, and chromatic details were represented using texture-based metrics as Homogeneity (HOM), Contrast (CON), and Entropy. In order to prepare the dataset for input into the machine learning model, the extracted features were saved as numerical scalars for every image. The feature extraction procedure is demonstrated in Fig. 3, which shows samples of the original drone image together with the ExG, CVI, and GCC that correspond to it [28], [29].

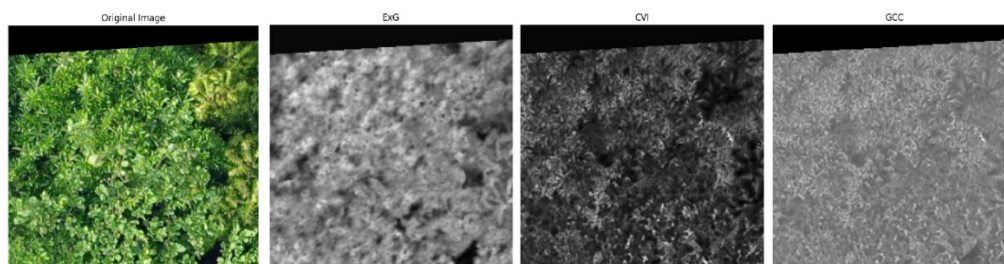


Fig. 3. Example dataset with color extraction result

To guarantee consistency among features, the scalar data was normalized before being fed into the Convolutional Neural Network (CNN) [30], [29], [28]. After that, the dataset was divided into 80% for training,

20%. This method guarantees that a significant amount of the data is used for model training while keeping enough data for validation to reliably evaluate the model's performance. According to the study, this split ratio aids in producing accurate forecasts and extending the model to new data, both of which are essential for evaluating carbon stocks in diverse settings [31].

2.3. Machine Learning Classifier

In order to categorize carbon stock levels based on both image data and scalar characteristics extracted from various indices and texture metrics, this study uses a multi-input Convolutional Neural Network (CNN) architecture in conjunction with a Multi-Layer Perceptron (MLP) [43], [44]. The MLP branch deals with scalar features that are taken from the dataset, whereas the CNN branch processes the image data (RGB images of size 224×224). For precise carbon stock categorization, this approach enables the model to efficiently incorporate both spatial and spectral information [45].

Three convolutional layers with 32, 64, and 128 filters make up the CNN branch. Its 3×3 kernel size allows it to effectively extract spatial data while lowering computing costs. A 2×2 max-pooling layer comes after each layer to reduce spatial dimensions, prevent overfitting, and preserve important features. ReLU activation is used to improve non-linearity and deal with vanishing gradient problems. Generalization is ensured by randomly deactivating neurons during training, with a dropout rate of 0.25 following each layer. To enable precise carbon stock categorization, the resultant feature maps are compressed into a one-dimensional vector for integration with the MLP branch. In investigations such as the identification of coconut palm disease, similar structures and dropout procedures have demonstrated better classification accuracy [46], [47].

Six features—Excess Green Index (ExG), Color Vegetation Index (CVI), Green Chromatic Coordinate (GCC), Homogeneity (HOM), Contrast (CON), and Entropy (ENT)—are processed by the MLP branch. These features were chosen because they are good at capturing the spectral and textural characteristics of vegetation. While HOM, Contrast, and ENT offer texture-based metrics on structural regularity, intensity variation, and randomness, ExG, CVI, and GCC use color bands to show the density and health of the vegetation. ReLU activation is used for non-linearity in two dense layers of 64 and 32 neurons, while batch normalization stabilizes and speeds up training. For accurate carbon stock categorization, a 0.5 dropout rate ensures robust integration of spectral and textural data by preventing overfitting [48], [49], [50].

A dense layer of 128 neurons comes after the fusion layer, which is made up of the concatenation of the CNN and MLP branch outputs. Lastly, the model uses a softmax activation function to generate a three-class classification output ("Low," "Medium," and "High"). The categorical cross-entropy loss function is minimized using the Adam optimizer, and overfitting is avoided by applying early halting with a 20-epoch patience. Five-fold cross-validation is used in the training phase to ensure a reliable model evaluation [43], [51].

This study creates seven unique models to examine the effects of specific variables and their combinations: Excess Green Index (ExG) is the scalar feature used by M1_exg, Color Vegetation Index (CVI) by M2_cvi, Green Chromatic Coordinate (GCC) by M3_gcc, Homogeneity (HOM) by M4_hom, Contrast (CON) by M5_con, Entropy (ENT) by M6_ent, and all six features combined by M7_all. Every model combines the RGB image data with the scalar features mentioned above. To ensure alignment with the selected feature for each scenario, the dataset is sliced into relevant subsets to prepare the scalar features [52].

Data augmentation for underrepresented classes ("Low" and "High") is done throughout the training process by applying transformations such rotation, shifting, zooming, and flipping. This improves the robustness of the model and guarantees a balanced dataset [46]. To evaluate each model's performance, evaluation measures such as accuracy, precision, recall, and F1-score are computed. According to the results, each feature makes a distinct contribution to classification accuracy; texture-based features, such M4_hom, frequently surpass individual color indices. Though there is still opportunity for development in feature integration techniques, the combined feature model (M7_all) offers insights into how features interact [43], [50].

2.4. Model Evaluation

Any classification activity must include model evaluation since it offers information on the effectiveness and dependability of the models being employed. The accuracy, recall, precision, F1-score, and confusion matrix are among the measures used to evaluate the performance of classification models.

The frequency with which a model accurately forecasts the result is known as accuracy [53], [54]. It is computed by taking the total number of guesses and dividing it by the number of right forecasts. Overall accuracy (OA) in image classification is the percentage of pixels that are properly identified. Although accuracy is simple to comprehend and offers a broad perspective on performance, it can be deceptive when datasets are

unbalanced. In these situations, a model may achieve high accuracy by accurately categorizing the minority classes but only predicting the majority class [53], [55].

Recall, sometimes referred to as sensitivity, gauges how well a model can locate all pertinent examples. It determines the percentage of real positive examples that the model accurately detects. Recall is calculated as:

$$Recall = \frac{TP}{TP + FN} \quad (1)$$

where TP stands for true positives (positive cases that were accurately predicted to be positive) and FN for false negatives (positive cases that were mistakenly projected to be negative) [53], [56]. When it comes to reducing false negatives, recall is very vital. The goal is to prevent missing any positive examples since, for instance, in medical diagnostics, it is crucial to identify all patients with a certain ailment, even if some healthy individuals are misdiagnosed.

Precision quantifies how well optimistic predictions work. It determines the percentage of expected positive cases that turn out to be actual positive.

$$Precision = \frac{TP}{TP+FP} \quad (2)$$

Above is the precision formula, where FP stands for false positives (negative cases that were mistakenly projected as positive) and TP is the number of true positives. In order to minimize false positives, precision is vital [53]. When determining whether an email is spam, for example, it is more crucial to prevent incorrectly labelling a crucial communication as spam than to identify every spam email.

The F1-score offers a balance between precision and recall by taking the harmonic mean of the two measures. The following is the formula:

$$F1 = 2 \times \frac{Precision \times Recall}{Precision + Recall} \quad (3)$$

When working with imbalanced datasets and minimizing both false positives and false negatives, the F1-score is especially helpful [56]. A higher F1-score indicates that the model is performing better at striking a balance between recall and precision. The macro F1-score, which gives an overall evaluation of the model's performance in multi-class classification scenarios, is the average F1-score for all classes.

A table that shows a classification model's performance is called a confusion matrix. The counts of true positives (TP), false positives (FP), true negatives (TN), and false negatives (FN) are displayed, along with a thorough analysis of the forecasts [57]. By highlighting the model's mistakes, the confusion matrix helps to clarify its advantages and disadvantages. In conclusion, accuracy gives a general indication of correctness, but it might be deceptive when dealing with unbalanced data. Finding all pertinent examples is the focus of recall, whereas the accuracy of positive predictions is the focus of precision [58]. A confusion matrix offers a thorough analysis of classification performance, and the F1-score effectively handles imbalanced classes by striking a compromise between precision and recall. Any classification model will be evaluated more thoroughly and robustly if these measures are used together [59], [60].

To improve the robustness of the model evaluation, a five-fold cross-validation procedure was used. This method helped create a reliable and scalable carbon stock categorization algorithm by converting visual information into scalar data [32], [33], [34], [35]. A five-fold cross-validation strategy was chosen to improve the model evaluation's resilience. The usefulness of five-fold cross-validation in improving model evaluation is supported by research. For example, a study on machine learning models for nitrate load prediction showed that k-fold cross-validation lowers bias in model evaluation and yields accurate performance estimates [36]. Compared to alternative validation techniques like holdout validation, five-fold cross-validation is a good fit for the size of the dataset used in this study and lessens the impact of data splits on performance measurements. This method ultimately helped create a reliable and scalable carbon stock categorization algorithm by converting visual information into scalar data [37]. This procedure highlights how crucial feature extraction and preprocessing are to converting unprocessed image data into useful scalar representations for machine learning [38]. Accurate categorization and analysis of carbon stocks were made possible by the extensive dataset that the generated scalar features gave CNN for training [39], [40]. This procedure highlights how crucial feature extraction and preprocessing are to converting unprocessed image data into useful scalar representations for machine learning. Accurate categorization and analysis of carbon stocks were made possible by the extensive dataset that the generated scalar features gave CNN for training [41], [38], [42].

3. RESULTS AND DISCUSSION

The research findings are presented in this section along with a detailed analysis of the outcomes of the models that were put into practice. The performance of several feature extraction techniques, such as ExG, CVI, and GCC, as well as texture-based features including homogeneity, contrast, and entropy, constitute the basis of the evaluation. The outcomes of distinct feature sets and their combinations are examined in order to pinpoint important trends, the method's advantages, and its drawbacks. In order to offer suggestions for future advancements, possible issues such as overfitting and class imbalance are also examined. To solve the flaws found and improve the model's performance, suggestions are made, one of which is the application of transfer learning.

3.1. Baseline Model

Table 3 displays the findings from the examination of the baseline model. For each class—Low, Medium, and High—precision, recall, F1-score, and support measures are used to assess the model. To give a general picture of the model's performance, the accuracy, macro average, and weighted average numbers are also displayed.

Table 3. Classification results for baseline model

	Precision	Recall	F1 Score	Support
Low	0.5400	0.7636	0.6279	110
Medium	0.8547	0.6063	0.7087	221
High	0.6835	0.7744	0.7255	133
Accuracy			0.6918	464
Macro Avg	0.6927	0.7148	0.6874	464
Weighted Avg	0.7292	0.6924	0.7029	464

The table indicates that the baseline model's performance differs for each class. With an F1-score of 0.72, the High class has the highest precision, while the Low class has the lowest, at 0.54. The model is more adept at identifying data from the High class than the other classes, as seen by the High class's greatest recall of 0.77. The baseline model's overall accuracy value is 0.69.

With precision, recall, and F1-score of 0.69, 0.71, and 0.69, respectively, macro averaging reveals that the model's performance is comparatively balanced across the classes. With an accuracy of 0.73 and an F1-score of 0.70, the weighted average, on the other hand, produces somewhat better findings, indicating the larger contribution of the class with more samples (Medium). These findings demonstrate that while the baseline model does a respectable job, it may still be improved, particularly in terms of recall for the Medium class and precision for the Low class.

3.2. Classification Results for Color Features

Using the three main vegetation indices—Excess Green Index (ExG), Color Vegetation Index (CVI), and Green Chromatic Coordinates (GCC)—this section investigates how well color-based characteristics work in carbon stock classification. The accuracy, precision, recall, and F1-score of the models trained on these features are summarized in Table 4 and the confusion matrix for each model is shown in Fig. 4.

Table 4. Classification results for Color Features

	Accuracy	Precision	Recall	F1 Score
M1_exg	0.7110	0.7190	0.7110	0.6930
M2_cvi	0.6940	0.7090	0.6940	0.6980
M3_gcc	0.6590	0.7270	0.6590	0.6200

Table 4 displays the classification results for models trained on the three primary vegetation indices: Green Chromatic Coordinate (GCC), Color Vegetation Index (CVI), and Excess Green Index (ExG). Fig. 4 displays the confusion matrices. The ExG-based model had the best overall accuracy of 0.7110 and the highest weighted average F1-score of 0.6930 among these indices. Strong classification performance is shown in the confusion matrix for ExG (Fig. 4, top left), especially in the "Medium" and "High" carbon stock classes. This better performance is explained by ExG's capacity to highlight green spectral components, which are highly associated with vegetative density and health and hence useful for differentiating carbon stock levels.

With an accuracy of 0.6940 and an F1-score of 0.6980, the CVI-based model again demonstrated encouraging performance, notably outperforming the "Low" carbon stock class (Fig. 4, top right). Its inability to distinguish between the "Medium" and "High" classes, however, led to somewhat worse performance than

ExG. The CVI's sensitivity to both red and green bands may be the cause of this limitation, as overlapping spectral responses impair the CVI's capacity to discriminate in these categories.

Out of the three indices, the GCC-based model showed the lowest F1-score (0.6200) and overall accuracy (0.659). Even though it performed worse, GCC had the highest precision of 0.7270 (Fig. 4, bottom), suggesting that it could be helpful in situations that need accurate classifications. GCC's weak sensitivity to changes in vegetation density, which are crucial for differentiating carbon stock levels, may be the cause of the decreased accuracy. These results imply that CVI and GCC might be complementing features, although ExG is the most successful independent color-based feature. To improve overall classification accuracy and resilience, future studies should investigate integrating these indices with additional characteristics or applying sophisticated fusion algorithms.

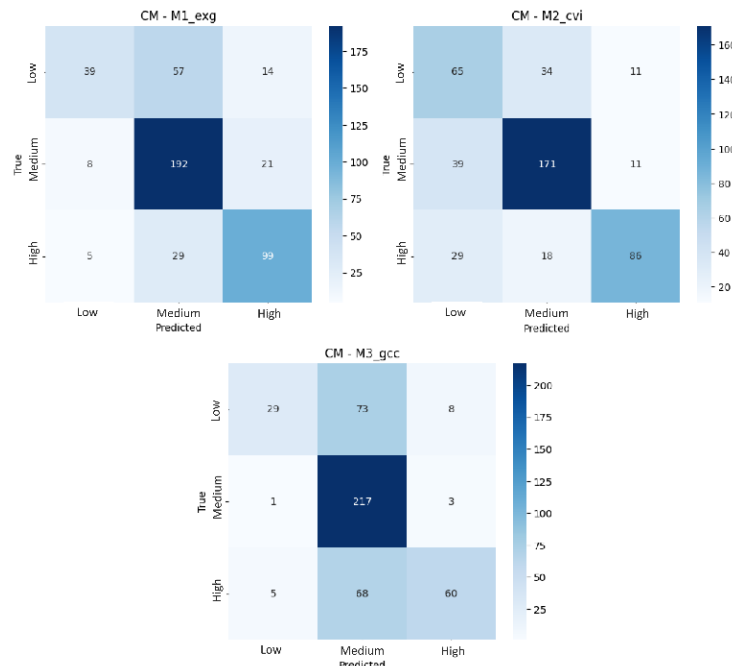


Fig. 4. Color features confusion matrix

3.3. Classification Results for Texture Features

The classification performance of scalar features, such as homogeneity, contrast, and entropy, was assessed using confusion matrices, classification reports, and accuracy measures. Understanding the function of these textural characteristics in distinguishing between carbon stock classes and determining their advantages and disadvantages in classification tasks were the main goals of this investigation. Table 5 provides specifics on the evaluation's findings.

Table 5. Classification results for Texture Features

	Accuracy	Precision	Recall	F1 Score
M4_hom	0.7070	0.7110	0.7070	0.6970
M5_con	0.6120	0.6910	0.6120	0.5480
M6_ent	0.6880	0.7210	0.6880	0.6710

The confusion matrices for models M4_hom, M5_con, and M6_ent are displayed in Fig. 5 to help further comprehend these findings. In the confusion matrix for M4_hom (Fig. 5, top left), every category shows consistent classification. In contrast to the other two models, the high carbon stock group benefits the most from a significant reduction in misclassification. It is implied that homogeneity as a characteristic can effectively represent the structural uniformity in the dataset.

Nonetheless, the confusion matrix for M5_con (Fig. 5, top right) shows a considerable level of misclassification, especially in the high carbon stock group, where many samples were mistakenly categorized as medium carbons. In particular, for higher levels, this result suggests that contrasts are not able to distinguish between various types of carbon stores.

Lastly, the confusion matrix of the entropy-based model (bottom, Fig. 5) performs admirably. Despite its challenges in correctly identifying low and high carbon stock classes, it has a respectable balance between groupings. Notwithstanding these drawbacks, entropy is still a valuable characteristic since it offers crucial details regarding structural complexity and randomness.

The study's results demonstrate that homogeneity is the most effective texture-based characteristic for carbon stock classification, as evidenced by a balanced confusion matrix and improved performance metrics. Entropy, which might be a complementary attribute, is more suited than contrast because of its restricted ability to distinguish between categories.

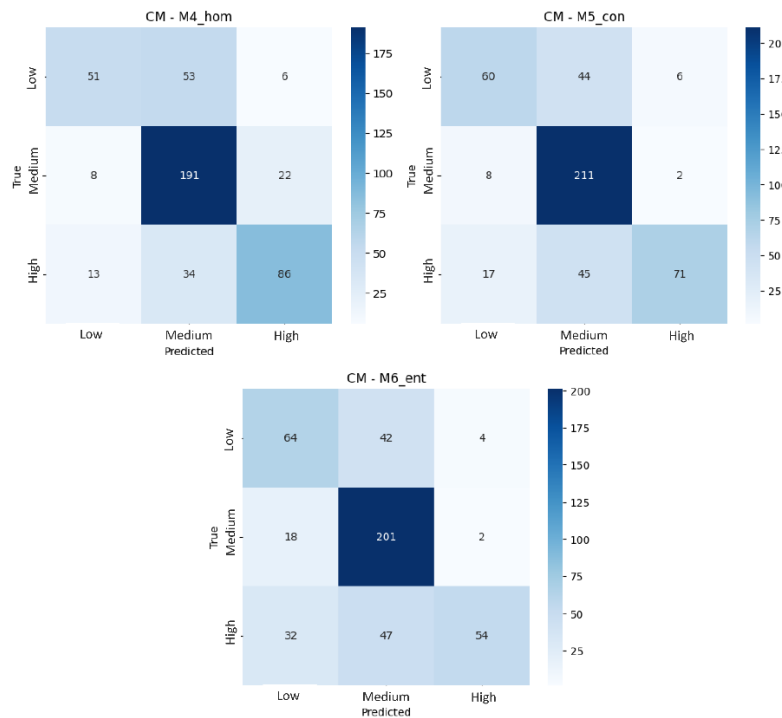


Fig. 5. Texture features confusion matrix

3.4. Classification Results for Combined Features

Utilizing the complementing advantages of both feature types, the combination feature model (M7_all) was created to increase classification accuracy for carbon stock categories by combining texture-based and color-based features. With an F1-score of 0.5480, accuracy of 0.6120, precision of 0.6910, and recall of 0.6120, M7_all's evaluation metrics are compiled in Table 6. The best individual models, including M4_hom (homogeneity) and M6_ent (entropy), outperformed the composite feature model, even though it contained a variety of information.

Table 6. Classification results for Texture Features

	Accuracy	Precision	Recall	F1 Score
M7_all	0.6120	0.6910	0.6120	0.5480

The confusion matrix for M7_all, which displays the comprehensive classification performance across the three carbon stock categories, is shown in Fig. 6. Based on these results, it can be seen that combining texture and color information into a single representation can be difficult. The model's strong categorization of the "Medium" carbon stock category is shown in the confusion matrix (Fig. 6); however, this matrix also shows striking misclassification in the "Low" and "High" categories, with many "High" samples incorrectly categorized as "Medium". This suggests that performance for more distinct categories may degrade as a result of the combination of texture and color data weakening the distinctive strength of certain attributes [61].

The constraints of the combined model may be due to redundant and overlapping feature distributions, which degrade the ability of texture and color features to discriminate. Although the class imbalance has been addressed with SMOTE, performance across all classes may be hampered by biases still present in the dataset. In addition, it is possible that complex correlations between spectral and spatial data are missed by combining

features directly. To effectively utilize the complementary capabilities of these features, future research should investigate sophisticated merging strategies such as attention processes or deep learning-based integration.

It is important to note that the results of this study are limited by the contextual and geographical limitations of the dataset - this dataset was only collected from Telkom University in Bandung, Indonesia. This geographical exclusivity raises questions regarding the generalizability of the model to other forest ecosystems with different vegetation patterns and biological conditions. The inaccuracy of the model classification, especially in the “Low” and “High” categories, may be due to the variation in spectral resolution and sensitivity produced by the mixture of drone footage and Google Earth Engine. In addition, the lack of a systematic sensitivity analysis to evaluate the robustness of the model under various conditions, such as alternative sensor types or environmental characteristics, limits the credibility of the results.

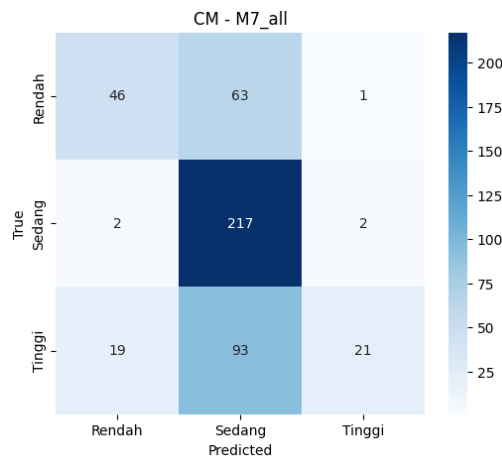


Fig. 6. Texture features confusion matrix

3.5. Model Comparison Across Scenarios

Performance of all models is compared in various feature extraction scenarios, such as the combined feature approach (M7_all), texture-based features (M4_hom, M5_con, M6_ent), and color-based features (M1_exg, M2_cvi, M3_gcc). The evaluation measures, such as accuracy, precision, recall, and F1-score, are listed in Table 7 and are used to determine the best approach for classifying carbon stocks.

Table 7. Classification results for Texture Features

Features	Accuracy	Precision	Recall	F1 Score
M1_exg Color-based	0.7110	0.7190	0.7110	0.6930
M2_cvi Color-based	0.6940	0.7090	0.6940	0.6980
M3_gcc Color-based	0.6590	0.7270	0.6590	0.6200
M4_hom Texture-based	0.7070	0.7110	0.7070	0.6970
M5_con Texture-based	0.6120	0.6910	0.6120	0.5480
M6_ent Texture-based	0.6880	0.7210	0.6880	0.6710
M7_all Combined	0.6120	0.6910	0.6120	0.5480

According to the results, the color-based model M3_gcc had the highest precision (0.7270), while the texture-based model M4_hom had the best accuracy (0.7070%). M6_ent's F1-score of 0.6710 indicated that it performed competitively as well. With an accuracy of 0.6120 and an F1-score of 0.5480, the combined model, M7_all, scored worse than the best individual models. These results imply that although the combined feature technique has potential, it is unable to fully utilize the advantages of distinct texture- and color-based features. Misclassifications are highlighted in the confusion matrix for M7_all, especially in the "Low" and "High" categories. This is probably because the feature distributions overlap and are redundant, which reduces discriminative power. Even though M7_all does not currently outperform the best single-feature models, it does demonstrate the potential advantages of incorporating complementary information [62].

A more thorough examination of the models' robustness and generalizability reveals some drawbacks. The study's dataset is unique to Telkom University in Bandung, Indonesia, which would limit the models' generalizability to other areas or forest types. Model performance may be impacted by changes in environmental factors like lighting or vegetation density. To determine wider application, future studies should

examine how well these models function in a variety of ecosystems, such as tropical, temperate, and boreal forests. Furthermore, sensitivity analyses incorporating differences in sensor kinds, resolutions, and preprocessing methods may offer a more thorough comprehension of the models' resilience in various scenarios.

The present findings are usefully contextualized by comparisons with earlier research. High-resolution photography is excellent for classifying carbon stocks, as evidenced by previous studies that used WorldView-3 and aerial laser scanning (ALS) data and produced R^2 values ranging from 0.68 to 0.85 for biomass estimating tasks [17]. Although the accuracy of the combined feature technique was not as high in this study, integrating textural and spectral data is still a potential way to improve classification results. By addressing the drawbacks of basic feature concatenation, advanced fusion techniques like attention-based processes or deep feature integration may be able to uncover the complimentary strengths of texture and color features.

To sum up, the comparison emphasizes how important it is to choose features that are suitable for certain carbon stock classification jobs [63]. More advanced feature fusion techniques that can successfully capture the connections between spectral and spatial information should be the main goal of future research in order to improve the combined feature model. Furthermore, improving oversampling methods like SMOTE and addressing residual dataset biases may enhance model performance for minority classes. Using transfer learning from previously trained models and investigating bigger, more varied datasets may also assist increase the results' generalizability. These developments could help the suggested methodology become a more reliable and scalable way to classify carbon stocks in various ecosystems and environmental settings.

4. CONCLUSION

Forests play a critical role in mitigating climate change by acting as carbon sinks, storing carbon dioxide from the atmosphere. This study introduces an integrated approach that combines spectral and textural features for carbon stock classification using UAV and GEE data.

With the best accuracy of 0.7070 and an F1-score of 0.6970, the results show that texture-based features—specifically, homogeneity and entropy—are the most successful in classifying carbon stocks. With an accuracy of 0.7110, the Excess Green Index model fared better than the others among color-based characteristics, while the Green Chromatic Coordinate model had the highest precision (0.7270). The difficulties in feature integration are highlighted by the mixed feature model (M7_all), which combines texture and color features, but only produced mediocre results.

This research makes two contributions. In theory, it offers a fresh paradigm for merging textural and spectral characteristics, which have historically been examined separately. This strategy closes the gap in earlier research by providing a scalable mechanism for classifying carbon stocks that can be used in a variety of forest ecosystems. In practice, the findings have been provided to Telkom University as additional information to help guide carbon-related policy choices, demonstrating the value of combining GEE and UAV data for environmental monitoring.

Nevertheless, the study has several limitations, including issues with feature integration and dataset size, the potential for overfitting, and the geographic constraint of relying solely on data from Telkom University. These limitations may impact the model's generalizability to other forest types or environmental conditions.

Future research should explore advanced fusion techniques, such as deep feature integration or transfer learning, to better leverage the complementary strengths of spectral and textural features. Expanding the dataset to include diverse geographic regions and addressing class imbalances could further enhance the model's robustness. Additionally, incorporating temporal and multispectral data may improve the scalability of the proposed approach for carbon stock estimation across varied ecosystems.

Acknowledgments

We extend our deepest gratitude to Telkom University for their invaluable support in facilitating this research, particularly in providing access to resources and data collection essential to the success of this project. We also acknowledge the contributions of the Sustainable Development Goals (SDGs) Center at Telkom University for their assistance in ensuring that this research aligns with sustainable practices and objectives

REFERENCES

- [1] Z. Yu, "Improved implicit diffusion model with knowledge distillation to estimate the spatial distribution density of carbon stock in remote sensing imagery," *arxiv*. 2024, [Online]. Available: <http://arxiv.org/abs/2411.17973>.
- [2] L. Zhang, Y. Cai, H. Huang, A. Li, L. Yang, and C. Zhou, "A CNN-LSTM Model for Soil Organic Carbon Content Prediction with Long Time Series of MODIS-Based Phenological Variables," *Remote Sens (Basel)*, vol. 14, no. 18, p. 4441, Sep. 2022, <https://doi.org/10.3390/rs14184441>.

- [3] L. J. R. Nunes, C. I. R. Meireles, C. J. Pinto Gomes, and N. M. C. Almeida Ribeiro, "Forest Contribution to Climate Change Mitigation: Management Oriented to Carbon Capture and Storage," *Climate*, vol. 8, no. 2, p. 21, Jan. 2020, <https://doi.org/10.3390/cli8020021>.
- [4] G. Reiersen *et al.*, "ReforesTree: A Dataset for Estimating Tropical Forest Carbon Stock with Deep Learning and Aerial Imagery," *arxiv*. 2022, [Online]. Available: <http://arxiv.org/abs/2201.11192>.
- [5] Y. Ye, M. Wang, L. Zhou, G. Lei, J. Fan, and Y. Qin, "Adjacent-Level Feature Cross-Fusion With 3-D CNN for Remote Sensing Image Change Detection," *IEEE Transactions on Geoscience and Remote Sensing*. 2023, <https://doi.org/10.1109/TGRS.2023.3305499>.
- [6] B. Pan *et al.*, "A CNN-LSTM Machine-Learning Method for Estimating Particulate Organic Carbon from Remote Sensing in Lakes," *Sustainability*, vol. 15, no. 17, p. 13043, Aug. 2023 <https://doi.org/10.3390/su151713043>.
- [7] A. R. Arunarani, S. Selvanayagi, M. S. Al Ansari, M. A. A. Walid, N. Devireddy, and M. M. Keerthi, "Crop Yield Prediction Using Spatio Temporal CNN and Multimodal Remote Sensing," in *2023 2nd International Conference on Edge Computing and Applications (ICECAA)*, pp. 1042–1048, 2023, <https://doi.org/10.1109/ICECAA58104.2023.10212267>.
- [8] S. Illarionova *et al.*, "A Survey of Computer Vision Techniques for Forest Characterization and Carbon Monitoring Tasks," *Remote Sensing*, vol. 14, no. 22, pp. 5861, 2022, <https://doi.org/10.3390/rs14225861>.
- [9] R. Su, W. Du, Y. Shan, H. Ying, W. Rihan, and R. Li, "Aboveground Carbon Stock Estimation Based on Backpack LiDAR and UAV Multispectral Imagery at the Forest Sample Plot Scale," *Remote Sens (Basel)*, vol. 16, no. 21, p. 3927, Oct. 2024, <https://doi.org/10.3390/rs16213927>.
- [10] I. Rahmatika, I. N. Hidayati, R. Suharyadi, and E. Nurjani, "Carbon Stock Estimation From Vegetation Biomass Using Spot-7 Imagery," *Indonesian Journal of Geography*, vol. 55, no. 3, pp. 385–396, 2023, <https://doi.org/10.22146/ijg.78690>.
- [11] S. F. Tóth, K. L. Oken, C. C. Stawitz, and H.-E. Andersen, "Optimal Survey Design for Forest Carbon Monitoring in Remote Regions Using Multi-Objective Mathematical Programming," *Forests*, vol. 13, no. 7, p. 972, Jun. 2022, <https://doi.org/10.3390/f13070972>.
- [12] A. O. Adegbite, I. Barrie, S. F. Osholake, T. Alesinloye, and A. B. Bello, "Artificial Intelligence in Climate Change Mitigation: A Review of Predictive Modeling and Data-Driven Solutions for Reducing Greenhouse Gas Emissions," *World Journal of Advanced Research and Reviews*, vol. 24, no. 1, pp. 408–414, Oct. 2024, <https://doi.org/10.30574/wjarr.2024.24.1.3043>.
- [13] A. A. Dar and N. Parthasarathy, "Patterns and drivers of tree carbon stocks in Kashmir Himalayan forests: implications for climate change mitigation," *Ecol Process*, vol. 11, no. 1, p. 58, Sep. 2022, <https://doi.org/10.1186/s13717-022-00402-z>.
- [14] C.-H. Lee, K.-Y. Chen, and L. D. Liu, "Effect of Texture Feature Distribution on Agriculture Field Type Classification with Multitemporal UAV RGB Images," *Remote Sens (Basel)*, vol. 16, no. 7, p. 1221, Mar. 2024, <https://doi.org/10.3390/rs16071221>.
- [15] K. Yang, H. Zhang, F. Wang, and R. Lai, "Extraction of Broad-Leaved Tree Crown Based on UAV Visible Images and OBIA-RF Model: A Case Study for Chinese Olive Trees," *Remote Sens (Basel)*, vol. 14, no. 10, p. 2469, May 2022, <https://doi.org/10.3390/rs14102469>.
- [16] K. C. L. Wong, L. Klein, A. F. da Silva, H. Wang, J. Singh, and T. Syeda-Mahmood, "Image-Based Soil Organic Carbon Remote Sensing from Satellite Images with Fourier Neural Operator and Structural Similarity," in *IGARSS 2023-2023 IEEE International Geoscience and Remote Sensing Symposium*, pp. 1305-1308, 2023, <https://doi.org/10.1109/IGARSS52108.2023.10281551>.
- [17] Y. Zhao, Y. Ma, L. J. Quackenbush, and Z. Zhen, "Estimation of Individual Tree Biomass in Natural Secondary Forests Based on ALS Data and WorldView-3 Imagery," *Remote Sens (Basel)*, vol. 14, no. 2, p. 271, Jan. 2022, <https://doi.org/10.3390/rs14020271>.
- [18] M. O. Duman and M. E. Tağluk, "Assessment of an Optimal Multilayer Perceptron Model in Estimation of Stock's Price Rates; a Sample from the Turkish Stock Exchange BIST," in *2024 8th International Artificial Intelligence and Data Processing Symposium (IDAP)*, pp. 1–5, 2024, <https://doi.org/10.1109/IDAP64064.2024.10710792>.
- [19] F. Ecer, S. Ardabili, S. S. Band, and A. Mosavi, "Training Multilayer Perceptron with Genetic Algorithms and Particle Swarm Optimization for Modeling Stock Price Index Prediction," *Entropy*, vol. 22, no. 11, p. 1239, Oct. 2020, <https://doi.org/10.3390/e22111239>.
- [20] B. Yuan, S. S. Sehra, and B. Chiu, "Multi-Scale and Multi-Network Deep Feature Fusion for Discriminative Scene Classification of High-Resolution Remote Sensing Images," *Remote Sens (Basel)*, vol. 16, no. 21, p. 3961, Oct. 2024, <https://doi.org/10.3390/rs16213961>.
- [21] D. Datta, M. Paul, M. Murshed, S. W. Teng, and L. M. Schmidtke, "Unveiling Soil-Vegetation Interactions: Reflection Relationships and an Attention-Based Deep Learning Approach for Carbon Estimation," in *2024 IEEE International Conference on Multimedia and Expo Workshops (ICMEW)*, pp. 1–6, 2024, <https://doi.org/10.1109/ICMEW63481.2024.10645460>.
- [22] L. Wang, J. Gao, and X. Geng, "A Modified Homotopy-Based Tensor Eigenpairs Algorithm for Remote Sensing Feature Extraction," *IEEE Geoscience and Remote Sensing Letters*, vol. 19, pp. 1–5, 2022, <https://doi.org/10.1109/LGRS.2021.3089153>.

- [23] R. Du, G. Wang, N. Zhang, L. Chen, and W. Liu, "Domain Adaptive Remote Sensing Scene Classification With Middle-Layer Feature Extraction and Nuclear Norm Maximization," *IEEE J Sel Top Appl Earth Obs Remote Sens*, vol. 17, pp. 2448–2460, 2024, <https://doi.org/10.1109/JSTARS.2023.3339336>.
- [24] Standar Nasional Indonesia, "Pengukuran dan penghitungan cadangan karbon-Pengukuran lapangan untuk penaksiran cadangan karbon berbasis lahan (land-based carbon accounting)," 2019. [Online]. Available: www.bsn.go.id.
- [25] "Strategi Nasional REDD+," 2010.
- [26] M. Varsha, B. Poornima, and P. Kumar, "A Machine Learning Technique for Rice Blast Disease Severity Prediction Using K-Means SMOTE Class Balancing," *Int J Risk Conting Manag*, vol. 11, no. 1, pp. 1–27, Dec. 2022, <https://doi.org/10.4018/IJRCM.315304>.
- [27] G. R. Patra, S. P. Iyer, S. Satyaprakash, and M. N. Mohanty, "A Class Balancing Based Machine Learning Approach for Fraudulent Credit Card Transaction Detection," in *2023 1st International Conference on Circuits, Power and Intelligent Systems (CCPIS)*, pp. 1–6, 2023, <https://doi.org/10.1109/CCPIS59145.2023.10291883>.
- [28] Z. Wu *et al.*, "Urban carbon stock estimation based on deep learning and UAV remote sensing: a case study in Southern China," *All Earth*, vol. 35, no. 1, pp. 272–286, Dec. 2023, <https://doi.org/10.1080/27669645.2023.2249645>.
- [29] B. Wang, Y. Chen, Z. Yan, and W. Liu, "Integrating Remote Sensing Data and CNN-LSTM-Attention Techniques for Improved Forest Stock Volume Estimation: A Comprehensive Analysis of Baishanzu Forest Park, China," *Remote Sens (Basel)*, vol. 16, no. 2, p. 324, Jan. 2024, <https://doi.org/10.3390/rs16020324>.
- [30] A. A. S. Gunawan, I. S. Edbert, F. S. Pramudya, and A. N. Rakhimah, "Web-based mangrove distribution and carbon stock monitoring system in Papua using CNN on satellite imagery," *Procedia Comput Sci*, vol. 245, pp. 637–646, 2024, <https://doi.org/10.1016/j.procs.2024.10.290>.
- [31] H. Mosaid *et al.*, "Improved soil carbon stock spatial prediction in a Mediterranean soil erosion site through robust machine learning techniques," *Environ Monit Assess*, vol. 196, no. 2, p. 130, Feb. 2024, <https://doi.org/10.1007/s10661-024-12294-x>.
- [32] H. Henri, A. M. Farhaby, O. Supratman, W. Adi, and S. Febrianto, "Assessment of species diversity, biomass and carbon stock of mangrove forests on Belitung Island, Indonesia," *Biodiversitas*, vol. 25, no. 1, Feb. 2024, <https://doi.org/10.13057/biodiv/d250103>.
- [33] I. P. Sugiana, T. Prartono, R. Rastina, and A. F. Koropitan, "Ecosystem carbon stock and annual sequestration rate from three genera-dominated mangrove zones in Benoa Bay, Bali, Indonesia," *Biodiversitas*, vol. 25, no. 1, Feb. 2024, <https://doi.org/10.13057/biodiv/d250133>.
- [34] J. Tang and J. Li, "Carbon risk and return prediction: Evidence from the multi-CNN method," *Front Environ Sci*, vol. 10, Oct. 2022, <https://doi.org/10.3389/fenvs.2022.1035809>.
- [35] J. Asian, N. D. Arianti, A. Ariefin, and M. Muslih, "Comparison of feature extraction and auto-preprocessing for chili pepper (*Capsicum Frutescens*) quality classification using machine learning," *IAES International Journal of Artificial Intelligence (IJ-AI)*, vol. 13, no. 1, p. 319, Mar. 2024, <https://doi.org/10.11591/ijai.v13.i1.pp319-328>.
- [36] K. Jung, D.-H. Bae, M.-J. Um, S. Kim, S. Jeon, and D. Park, "Evaluation of Nitrate Load Estimations Using Neural Networks and Canonical Correlation Analysis with K-Fold Cross-Validation," *Sustainability*, vol. 12, no. 1, p. 400, Jan. 2020, <https://doi.org/10.3390/su12010400>.
- [37] B. Kumar, K. Manisha, A. Sinha, A. Kumar, and J. Kumar, "Deep Learning Based Image Classification for Automated Face Spoofing Detection Using Machine Learning: Convolutional Neural Network," in *2024 2nd World Conference on Communication & Computing (WCONF)*, pp. 1–8, 2024, <https://doi.org/10.1109/WCONF61366.2024.10692150>.
- [38] S. A. Mosa, Istomo, and A. P. P. Hartoyo, "Estimation of vegetation density using NDVI and carbon stock in the Utilization Zone of Gunung Halimun Salak National Park," *IOP Conf Ser Earth Environ Sci*, vol. 1315, no. 1, p. 012041, Mar. 2024, <https://doi.org/10.1088/1755-1315/1315/1/012041>.
- [39] F. Zhang, Z. Hu, K. Yang, Y. Fu, Z. Feng, and M. Bai, "The Surface Crack Extraction Method Based on Machine Learning of Image and Quantitative Feature Information Acquisition Method," *Remote Sens (Basel)*, vol. 13, no. 8, p. 1534, Apr. 2021, <https://doi.org/10.3390/rs13081534>.
- [40] M. E. Sahin, "Image processing and machine learning-based bone fracture detection and classification using X-ray images," *Int J Imaging Syst Technol*, vol. 33, no. 3, pp. 853–865, May 2023, <https://doi.org/10.1002/ima.22849>.
- [41] P. P. Monfared and S. M. Jarchi, "CNN-NLP Based Persian Feedback Detection of Stock Symbols in the Stock Market," in *2024 10th International Conference on Artificial Intelligence and Robotics (QICAR)*, pp. 125–130, 2024, <https://doi.org/10.1109/QICAR61538.2024.10496608>.
- [42] H. I. Tuncer and D. Altinel, "Classification of Eye Diseases using Machine Learning with Preprocessing," in *2024 8th International Artificial Intelligence and Data Processing Symposium (IDAP)*, pp. 1–7, 2024, <https://doi.org/10.1109/IDAP64064.2024.10710977>.
- [43] X. Zong, "MLP, CNN, LSTM and Hybrid SVM for Stock Index Forecasting Task to INDU and FTSE100," *SSRN Electronic Journal*, 2020, <https://doi.org/10.2139/ssrn.3644034>.
- [44] A. Sharma and S. Rani, "A Cutting-Edge Hybrid Deep Learning Technique with Low Rank Approximation for Attacks Classification on <sc>IoT</sc> Traffic Data," *Internet Technology Letters*, Nov. 2024, <https://doi.org/10.1002/itl2.606>.
- [45] D. S. Rao, K. M. Lakshmi, M. Sridevi, P. P. M. Krishna, G. J. Rao "Multi-Object Classification for Deep Learning Analysis in CNN and MLP," *NeuroQuantology*, vol. 20, no. 10, p. 5805, 2022, <https://doi.org/10.48047/nq.2022.20.10.NQ55581>.

- [46] P. Mittal, A. Sharma, and R. Singh, "Deformable patch-based-multi-layer perceptron Mixer model for forest fire aerial image classification," *J Appl Remote Sens*, vol. 17, no. 2, Nov. 2022, <https://doi.org/10.1117/1.JRS.17.022203>.
- [47] D. Banerjee, V. Kukreja, S. Vats, V. Jain, and B. Goyal, "Enhancing Accuracy of Yellowing Disease Severity Level Detection in Coconut Palms with SVM Regularization and CNN Feature Extraction," in *2023 Third International Conference on Secure Cyber Computing and Communication (ICSCCC)*, pp. 109–114, 2023, <https://doi.org/10.1109/ICSCCC58608.2023.10176557>.
- [48] F. Guo, D. Liu, S. Mo, Q. Li, J. Meng, and Q. Huang, "Assessment of Phenological Dynamics of Different Vegetation Types and Their Environmental Drivers with Near-Surface Remote Sensing: A Case Study on the Loess Plateau of China," *Plants*, vol. 13, no. 13, p. 1826, Jul. 2024, <https://doi.org/10.3390/plants13131826>.
- [49] K. A. Rashedi, M. T. Ismail, S. Al Wadi, A. Serroukh, T. S. Alshammari, and J. J. Jaber, "Multi-Layer Perceptron-Based Classification with Application to Outlier Detection in Saudi Arabia Stock Returns," *Journal of Risk and Financial Management*, vol. 17, no. 2, p. 69, Feb. 2024, <https://doi.org/10.3390/jrfm17020069>.
- [50] C. Wang *et al.*, "R-MFNet: Analysis of Urban Carbon Stock Change against the Background of Land-Use Change Based on a Residual Multi-Module Fusion Network," *Remote Sens (Basel)*, vol. 15, no. 11, Jun. 2023, <https://doi.org/10.3390/rs15112823>.
- [51] Y. Zheng, Z. Dang, C. Peng, C. Yang, and X. Gao, "Multi-view Multi-label Anomaly Network Traffic Classification based on MLP-Mixer Neural Network," arXiv preprint arXiv:2210.16719, 2022, <https://doi.org/10.48550/arXiv.2210.16719>.
- [52] Q. Zhang, E. Bai, M. Shao, and H. Liang, "Video-Mlp: Convolution-Free, Attention-Free Architecture for Video Classification," *Journal of Intelligent & Fuzzy Systems, (Preprint)*, pp. 1-12, 2023, <https://doi.org/10.2139/ssrn.4372886>.
- [53] S. Illarionova, P. Tregubova, I. Shukhratov, D. Shadrin, A. Efimov, and E. Burnaev, "Advancing forest carbon stocks' mapping using a hierarchical approach with machine learning and satellite imagery," *Sci Rep*, vol. 14, no. 1, Dec. 2024, <https://doi.org/10.1038/s41598-024-71133-8>.
- [54] T. Leditznig and H. Klug, "Estimating Carbon Stock in Unmanaged Forests Using Field Data and Remote Sensing," *Remote Sens (Basel)*, vol. 16, no. 21, p. 3926, Oct. 2024, <https://doi.org/10.3390/rs16213926>.
- [55] T. D. Pham *et al.*, "Advances in Earth observation and machine learning for quantifying blue carbon," *Earth-Science Reviews*, p. 104501, 2023, <https://doi.org/10.1016/j.earscirev.2023.104501>.
- [56] R. Ma, W. Wu, Q. Wang, N. Liu, and Y. Chang, "Offshore Hydrocarbon Exploitation Target Extraction Based on Time-Series Night Light Remote Sensing Images and Machine Learning Models: A Comparison of Six Machine Learning Algorithms and Their Multi-Feature Importance," *Remote Sens (Basel)*, vol. 15, no. 7, Apr. 2023, <https://doi.org/10.3390/rs15071843>.
- [57] L. Dong *et al.*, "Application of convolutional neural network on lei bamboo above-ground-biomass (AGB) estimation using Worldview-2," *Remote Sens (Basel)*, vol. 12, no. 6, Mar. 2020, <https://doi.org/10.3390/rs12060958>.
- [58] D. Krstinić, M. Braović, L. Šerić, and D. Božić-Štulić, "Multi-label Classifier Performance Evaluation with Confusion Matrix," in *Computer Science & Information Technology*, pp. 1–14, 2020, <https://doi.org/10.5121/csit.2020.100801>.
- [59] X. Zhou and A. Del Valle, "Range Based Confusion Matrix for Imbalanced Time Series Classification," in *2020 6th Conference on Data Science and Machine Learning Applications (CDMA)*, pp. 1–6, 2020, <https://doi.org/10.1109/CDMA47397.2020.00006>.
- [60] I. O. Awoyelu, B. R. Ojo, S. B. Aregbesola, O. O. Soyele "Performance Evaluation of a Classification Model for Oral Tumor Diagnosis," *Computer and Information Science*, vol. 13, no. 1, p. 1, Dec. 2019, <https://doi.org/10.5539/cis.v13n1p1>.
- [61] A. Shandilya, "ML Model for Stock Classification," *Int J Res Appl Sci Eng Technol*, vol. 12, no. 4, pp. 5230–5239, Apr. 2024, <https://doi.org/10.22214/ijraset.2024.61136>.
- [62] J. Zhou *et al.*, "Evaluation of Different Algorithms for Estimating the Growing Stock Volume of Pinus massoniana Plantations Using Spectral and Spatial Information from a SPOT6 Image," *Forests*, vol. 11, no. 5, p. 540, May 2020, <https://doi.org/10.3390/f11050540>.
- [63] A. Algherairy, W. Almatarr, E. Bakri, and S. Albelali, "The Impact of Feature Selection on Different Machine Learning Models for Breast Cancer Classification," in *2022 7th International Conference on Data Science and Machine Learning Applications (CDMA)*, pp. 91–96, 2022, <https://doi.org/10.1109/CDMA54072.2022.00020>.

BIOGRAPHY OF AUTHORS



Raditya Aydin, an Informatics student at Telkom University and CHRO at Redooceit, leads a startup utilizing IoT to process organic waste into maggot for animal feed. Redooceit won the "Best Category" award in Innovillage 2023 for Zero Waste Solutions and actively trains Lengkong Village residents in organic waste management. Raditya is also part of the Programming Club (Proclub) at Telkom University. More details: GitHub: <https://github.com/Radiit/>, Email: radityaaydin@student.telkomuniversity.ac.id.



Erwin Budi Setiawan, an Associate Professor at Telkom University's Faculty of Informatics, specializes in people analytics, social media analysis, and machine learning, with over a decade of research and teaching experience. He earned his undergraduate, graduate, and doctoral degrees from Bandung Institute of Technology. With over 1,300 citations, his work has significantly contributed to sentiment analysis, online hoax and hate speech detection, and social media information reliability. To further the subject of informatics, Dr. Setiawan also works with other researchers and actively mentors students. Email: erwinbudisetiawan@telkomuniversity.ac.id, orcid: 0000-0002-2121-8776.